

Free vibration analysis of concrete arch dams by quadratic ideal-coupled method

Mohammad Rezaiee-Pajand*, Ahmad Aftabi Sani and Mohammad Sadegh Kazemiyari

Department of Civil Engineering, Ferdowsi University of Mashhad, Mashhad, Iran

(Received April 5, 2017, Revised October 15, 2017, Accepted October 23, 2017)

Abstract. This paper is devoted to two new techniques for free vibration analysis of concrete arch dam-reservoir systems. The proposed schemes are quadratic ideal-coupled eigen-problems, which can solve the originally non-symmetric eigen-problem of the system. To find the natural frequencies and mode shapes, a new special-purpose eigen-value solution routine is developed. Moreover, the accuracy of the proposed approach is thoroughly assessed, and it is confirmed that the new scheme is very accurate under all practical conditions. It is also concluded that both decoupled and ideal-coupled strategy proposed in the previous works can be considered as special cases of the current more general procedure.

Keywords: arch dam; fluid-structure interaction; decoupled method; ideal-coupled method; quadratic ideal-coupled method; subspace iteration method

1. Introduction

The dynamic behavior of concrete arch dam-reservoir systems can be thoroughly investigated by the finite element approach. Generally, the dynamic analysis may be conducted in time or frequency domains. Note that; dynamic analysis may be carried out in these domains either by direct scheme or modal method. Hence, finding the natural frequencies and corresponding mode shapes of the arch dam plays an important role in the dynamic analysis. To find natural frequencies and mode shapes, it is required to solve the eigen-value problem governing the free vibration of the dam-reservoir system.

In usual, the dam is discretized by the solid finite elements, and the reservoir is discretized with the help of the fluid finite elements. Displacements are the variables in the solid, while various choices are available for the discretization of the fluid into volume elements. The unknown variable could be a vector field of fluid-particle displacements (Bathe and Hahn 1979), or a scalar field such as the pressure, velocity potential or displacement potential (Bouaanani and Lu 2009). The former formulation is named Lagrangian method, and the latter is entitled Eulerian approach (Zienkiewicz and Bettess 1978). A displacement based fluid field can be easily implemented in the common finite element codes.

Additionally, this formulation leads to a symmetric vibration problem. Nonetheless, usage of this formulation substantially increases the fluid degrees of freedom as compared to the scalar field formulations. As a consequence, a large number of spurious eigen-modes which correspond to rotational fluid motions of zero

frequencies emerge. These modes cause difficulties in calculating the natural frequencies (Felippa 1985). Employing scalar fields automatically satisfy the irrotational condition of the fluid motions. As a result, the spurious-mode problem is remedied. Moreover, the number of required degrees of freedom is minimized. In this formulation, the corresponding vibration eigen-problem is formally non-symmetric. Extensive research has been conducted to symmetrize this eigen-value problem. In what follows, the previous corresponding literature is briefly reviewed.

Morand and Ohayon (1979) took advantage of a three-field mixed variational formulation. In this way, they achieved a symmetric form of the aforementioned problem. It should be noted that pressure and displacement potential were considered as the unknowns in the fluid domain. Everstine (1981) presented a symmetric formulation in which velocity potential was the primary variable of the fluid domain. In this technique, the eigen-problem consisted of three matrices even for un-damped systems. Consequently, this algorithm was efficient for damped ones. Additionally, this approach was not able to compute the hydrostatic pressure. Besides, Geradin *et al.* (1984) used displacement potential. As a result, they gained a standard eigen-value problem. Afterwards, Olson and Bathe (1985) employed hydrostatic pressure and velocity potential as the unknown fields of the fluid domain. Consequently, they symmetrized the above-cited eigen-problem. Afterwards, Felippa (1985) suggested eight symmetrical forms. In another work, this researcher employed matrix augmentation and static condensation to reach the aforesaid eight symmetrical forms (Felippa 1988). Olson and Vandini (1989) applied displacement, velocity potential and hydrostatic pressure as unknowns in fluid-structure problems. At the next stage, they condensed out the hydrostatic pressure. In this way, they achieved a symmetric

*Corresponding author, Professor
E-mail: rezaiee@um.ac.ir

quadratic eigen-value problem. Kayser-Herold and Matthies (2005) used the first-order least squares finite element method instead of the Galerkin approaches for formulating the fluid-structure interaction problem. In this way, they achieved symmetric positive definite matrices.

Sandberg (1995) took advantage of the eigen-vectors of each domain for presenting a new symmetric version of the originally non-symmetric coupled eigen-problem, which employed displacement finite element formulation for the solid and either pressure or displacement potential for the fluid. This strategy was the advent of developing new generation of symmetrizing approaches in which coupled modes shapes are not employed. Similarly, Lotfi (2005) employed decoupled mode shapes instead of the coupled ones in the modal analysis. With the help of this innovative procedure, it was not required to solve the non-symmetric coupled eigen-problem. In this method, the decoupled mode shapes were envisaged as the Ritz vectors. It should be reminded that the decoupled eigen-problems are symmetric. Afterwards, some researchers compared the capability of the decoupled scheme with the coupled one (Samii and Lotfi 2007). Then, Aftabi Sani and Lotfi (2010) utilized new mode shapes entitled ideal-coupled modes in the modal analysis of concrete arch dams. These modes were applied in a similar manner to the decoupled modes. Nevertheless, they were actually coupled mode shapes of two ideal fictitious systems. It is worth emphasizing that the coupled eigen-problem of these systems were symmetric. Then, Hojati and Lotfi (2011) used semi-infinite fluid elements for dynamic analysis of gravity dams, and they proposed a fast simple procedure for calculating the impedance matrix of these elements. Furthermore, Aftabi Sani and Lotfi (2011) suggested a new efficient technique for evaluating the earthquake response of concrete arch dams. In this work, the dam-reservoir-foundation interaction effects were considered. Additionally, Chopra (2012) identified the factors which played significant roles in the three-dimensional analysis of arch dams.

In this paper, new quadratic-symmetric shapes of the corresponding non-symmetric eigen-value problem are presented. Authors' formulation improves the accuracy of the ideal-coupled technique. To solve these quadratic eigen-value problems, a novel eigen-value solution routine is developed.

The remaining text is organized as follows. Section 2 deals with the governing equation of the dam-reservoir system. It should be noted that nodal pressures and displacements are considered as the unknowns of the fluid and solid domain, respectively. Then, the free vibration equations are presented. Afterwards, previously proposed forms of the corresponding eigen-value problem are mentioned. In section 3, new symmetric quadratic forms of this problem are formulated. Section 4 briefly reviews the methods which can be used to solve the quadratic eigen-value problems. In section 5, a novel approach is developed for solving the suggested quadratic eigen-value problems. Numerical samples corroborate the robustness and efficiency of the new approach in section 6. Finally, the conclusions are summarized in Section 7.

2. Governing equations

The dam with a finite reservoir is discretized by utilizing the finite element scheme. The coupled equation of the system has the following appearance with displacement and pressure degrees of freedom for solid and fluid domains, respectively (Aftabi S. and Lotfi 2010)

$$\begin{bmatrix} \mathbf{M} & \mathbf{0} \\ \mathbf{B} & \mathbf{G} \end{bmatrix} \begin{bmatrix} \ddot{\mathbf{r}} \\ \ddot{\mathbf{p}} \end{bmatrix} + \begin{bmatrix} \mathbf{C} & \mathbf{0} \\ \mathbf{0} & \mathbf{L} \end{bmatrix} \begin{bmatrix} \dot{\mathbf{r}} \\ \dot{\mathbf{p}} \end{bmatrix} + \begin{bmatrix} \mathbf{K} & -\mathbf{B}^T \\ \mathbf{0} & \mathbf{H} \end{bmatrix} \begin{bmatrix} \mathbf{r} \\ \mathbf{p} \end{bmatrix} = \begin{bmatrix} -\mathbf{M}\mathbf{J}\mathbf{a}_g \\ -\mathbf{B}\mathbf{J}\mathbf{a}_g \end{bmatrix} \quad (1)$$

In this equation, the mass, stiffness and damping matrix of the dam body are denoted by \mathbf{M} , \mathbf{K} and \mathbf{C} , respectively. In addition, \mathbf{G} , \mathbf{H} and \mathbf{L} are the generalized mass, stiffness and damping of fluid domain, correspondingly. Moreover, \mathbf{B} is the interaction matrix. The unknown vectors of the problem are the nodal displacements and pressures which are stored in vector \mathbf{r} and \mathbf{p} , respectively. Furthermore, \mathbf{J} has three columns and number of nodal degrees of freedom rows, and it is made of 3×3 identity matrix. Note that; each column of this matrix is associated with a unit rigid body motion in cross-canyon, stream and vertical direction. Moreover, \mathbf{a}_g is the vector of ground accelerations. By performing the Fourier transform, the matrix Eq. (1) can be rewritten in the next form

$$\begin{bmatrix} -\omega^2 \mathbf{M} + \mathbf{K}(1 + 2\beta_d i) & -\mathbf{B}^T \\ -\omega^2 \mathbf{B} & -\omega^2 \mathbf{G} + i\omega \mathbf{L} + \mathbf{H} \end{bmatrix} \begin{bmatrix} \mathbf{r} \\ \mathbf{p} \end{bmatrix} = \begin{bmatrix} -\mathbf{M}\mathbf{J}\mathbf{a}_g \\ -\mathbf{B}\mathbf{J}\mathbf{a}_g \end{bmatrix} \quad (2)$$

In this relation, i is the imaginary unit, and ω denotes the natural frequency of the system. Recall that, the hysteretic damping matrix is employed in the aforesaid relationship. This matrix is related to the stiffness matrix as follows

$$\mathbf{C} = \frac{2\beta_d}{\omega} \mathbf{K} \quad (3)$$

in which β_d is the constant hysteretic factor of the dam body. It is worth emphasizing that Eq. (2) is the coupled equation of a dam with the finite reservoir system in the frequency domain.

2.1 Free vibration analysis

The eigen-problem corresponding to Eq. (2) has the subsequent shape (Rezaiee-Pajand *et al.* 2016)

$$\left(\omega^2 \begin{bmatrix} \mathbf{M} & \mathbf{0} \\ \mathbf{B} & \mathbf{G} \end{bmatrix} + \begin{bmatrix} -\mathbf{K} & \mathbf{B}^T \\ \mathbf{0} & -\mathbf{H} \end{bmatrix} \right) \begin{bmatrix} \mathbf{r} \\ \mathbf{p} \end{bmatrix} = \begin{bmatrix} \mathbf{0} \\ \mathbf{0} \end{bmatrix} \quad (4)$$

Obviously, this equality is analogous to the free vibration equation of un-damped systems. It is clear that the aforementioned eigen-value problem is linear and unsymmetric. For finding the eigen-pairs, the above-cited

relationship and some variation of it can be employed. Although, it is preferred to solve the actual coupled equation of the dam-reservoir system, there are several more efficient alternatives, which will be introduced in the following sub-sections.

2.2 Coupled eigen-problem

The actual coupled mode shapes and natural frequencies can be achieved by directly solving the original eigen-value problem presented in Eq. (4). These eigen-vectors are very appropriate for modal analysis. Generally, usage of these mode shapes results in more accurate responses. Due to the unsymmetry of the aforesaid equation, standard eigen-value solvers cannot be employed for finding the corresponding eigen-pairs. Other researchers have concluded that the unsymmetrical eigen-solvers are normally very time-consuming and complicated from computer programming point of view (Zienkiewicz and Bettess 1978, Felippa 1985, Sandberg 1995, Samii and Lotfi 2007, Aftabi and Lotfi 2010). It should be added that some methods symmetrize this problem by applying simplifying assumptions. In what follows, these techniques are introduced.

2.3 Decoupled eigen-problem

By omitting the interaction matrix \mathbf{B} , a symmetric variation of the original eigen-value problem can be achieved. This new shape of the actual problem is referred to as the “decoupled” form, and it has the next appearance

$$\left(\omega^2 \begin{bmatrix} \mathbf{M} & \mathbf{0} \\ \mathbf{0} & \mathbf{G} \end{bmatrix} - \begin{bmatrix} \mathbf{K} & \mathbf{0} \\ \mathbf{0} & \mathbf{H} \end{bmatrix} \right) \begin{bmatrix} \mathbf{r} \\ \mathbf{p} \end{bmatrix} = \begin{bmatrix} \mathbf{0} \\ \mathbf{0} \end{bmatrix} \quad (5)$$

Obviously, this eigen-problem is symmetric. Hence, it is possible to solve the current linear problem by applying the standard eigen-value solution routines. It is worthwhile to highlight that the eigen-vectors obtained from these symmetric equations are not the true mode shapes of the system. Nevertheless, they can be utilized in modal analysis approach named “decoupled modal strategy”. It should be remarked that these vectors can be considered as the Ritz vectors. As a consequence, it can be demonstrated that the usage of all decoupled modes yields exact answers. The natural frequencies calculated from the decoupled eigen-problem are not the eigen-values of the coupled dam-reservoir system. They are the natural frequencies of the dam and reservoir separately (Lotfi 2005, Aftabi and Lotfi 2010).

2.4 Ideal-coupled eigen-problem

This eigen-value problem is based on two ideal eigen-problems which are related to incompressible fluid and massless solid cases. The natural frequencies obtained from this method are closer to the original coupled eigen-values, in comparison to the decoupled ones. Additionally, the corresponding mode shapes are more similar to the actual ones. Therefore, usage of the ideal coupled eigen-vectors in the modal analysis leads to more accurate results, in comparison with the decoupled ones. The simplified form

of the first ideal eigen-problem has the following shape (Aftabi and Lotfi 2010)

$$(\omega^2(\mathbf{M} + \mathbf{M}_a) - \mathbf{K})\mathbf{r} = \mathbf{0} \quad (6)$$

in which \mathbf{M}_a is referred to as the added mass matrix and has the following appearance

$$\mathbf{M}_a = \mathbf{B}^T \mathbf{H}^{-1} \mathbf{B} \quad (7)$$

The pressure vector can be computed by using the next equation

$$\mathbf{p} = \omega^2 \mathbf{H}^{-1} \mathbf{B} \mathbf{r} \quad (8)$$

It is clear that the size of this eigen-problem is equal to the number of the unknown nodal displacements. The second ideal eigen-value problem can be expressed as below

$$(\omega^2(\mathbf{G} + \mathbf{G}_a) - \mathbf{H})\mathbf{p} = \mathbf{0} \quad (9)$$

where \mathbf{G}_a is defined as the next form

$$\mathbf{G}_a = \mathbf{B} \mathbf{K}^{-1} \mathbf{B}^T \quad (10)$$

The displacement vector can be calculated by employing the following relation

$$\mathbf{r} = \mathbf{K}^{-1} \mathbf{B}^T \mathbf{p} \quad (11)$$

Obviously, the size of the second ideal eigen-value problem is equal to the number of unknown nodal pressures of the fluid domain.

It is worthwhile to mention that the elimination of matrix \mathbf{M}_a and \mathbf{G}_a from Eqs. (6) and (9) leads to the decoupled eigen-value problem. As a consequence, the decoupled form of the actual eigen-problem is a special case of the ideal-coupled one.

The two aforementioned ideal eigen-problems can be expressed in the below shape

$$\begin{bmatrix} \omega^2(\mathbf{M} + \mathbf{M}_a) - \mathbf{K} & \mathbf{0} \\ \mathbf{0} & \omega^2(\mathbf{G} + \mathbf{G}_a) - \mathbf{H} \end{bmatrix} \begin{bmatrix} \mathbf{r} \\ \mathbf{p} \end{bmatrix} = \begin{bmatrix} \mathbf{0} \\ \mathbf{0} \end{bmatrix} \quad (12)$$

Clearly, this eigen-problem is symmetric. Hence, it can be solved with the help of standard common methods. It is worth emphasizing that the ideal-coupled technique is more accurate than the decoupled scheme (Aftabi S. and Lotfi 2010).

3. New quadratic ideal-coupled eigen-problem

Herein, a new alternative for the aforementioned eigen-problem is introduced. It will be demonstrated that the suggested strategy is more accurate than the ideal-coupled eigen-problem. In fact, both decoupled and ideal-coupled strategy proposed in the previous works can be considered as special cases of the current more general procedure. Furthermore, authors' scheme is based on two different

quadratic eigen-value problems, which are separately discussed in this section.

Considering the lower partition equation of Eq. (4) and solving the pressure vector in terms of the displacement vector leads to the succeeding result

$$\mathbf{p} = \omega^2 (\mathbf{H} - \omega^2 \mathbf{G})^{-1} \mathbf{B} \mathbf{r} \quad (13)$$

It is worthwhile to highlight that Eq. (8) is the approximate form of this equality in which \mathbf{G} is omitted. Note that; Eq. (8) is one of the key formulas applied in the ideal-coupled strategy. Clearly, $(\mathbf{H} - \omega^2 \mathbf{G})$ is the subtraction of two matrices, which should be inverted in the right side of the latter relationship. By utilizing the first-order approximation of the Taylor series, this matrix inversion can be calculated as below (Rezaiee-Pajand and Kazemiyani 2014, Rezaiee-Pajand *et al.* 2014)

$$(\mathbf{H} - \omega^2 \mathbf{G})^{-1} \cong \mathbf{H}^{-1} + \omega^2 \mathbf{H}^{-1} \mathbf{G} \mathbf{H}^{-1} \quad (14)$$

Inserting this equation into the Eq. (13) results in the next relationship

$$\mathbf{p} \cong \omega^2 (\mathbf{H}^{-1} + \omega^2 \mathbf{H}^{-1} \mathbf{G} \mathbf{H}^{-1}) \mathbf{B} \mathbf{r} \quad (15)$$

Substituting the latter equality into the upper partition equation of Eq. (4) leads to the subsequent result

$$(\omega^4 \mathbf{Q} \mathbf{G} \mathbf{Q}^T + \omega^2 (\mathbf{M} + \mathbf{M}_a) - \mathbf{K}) \mathbf{r} = \mathbf{0} \quad (16)$$

where

$$\mathbf{Q} = \mathbf{B}^T \mathbf{H}^{-1} \quad (17)$$

Actually, neglecting the first term of Eq. (16) leads to Eq. (6) in the ideal-coupled tactic. This fact shows that the first form of the ideal-coupled approach is a special case of the first quadratic ideal-coupled technique. Obviously, the size of this quadratic eigen-problem is equal to the number of unknown nodal displacement.

Subsequently, the second quadratic ideal eigen-problem is constructed. For this purpose, the displacement vector is solved in terms of the pressure vector by employing the upper partition equation of Eq. (4). The achieved displacement vector can be expressed as follows

$$\mathbf{r} = (\mathbf{K} - \omega^2 \mathbf{M})^{-1} \mathbf{B}^T \mathbf{p} \quad (18)$$

In fact, Eq. (18) is the exact form of Eq. (11) in which \mathbf{M} is neglected. Recall that, Eq. (11) plays an important role in the ideal-coupled technique. Analogously, $(\mathbf{K} - \omega^2 \mathbf{M})$ can be inverted by using the first-order approximation of the Taylor series as below

$$(\mathbf{K} - \omega^2 \mathbf{M})^{-1} \cong \mathbf{K}^{-1} + \omega^2 \mathbf{K}^{-1} \mathbf{M} \mathbf{K}^{-1} \quad (19)$$

Introducing this equation into Eq. (18) leads to the next equality

$$\mathbf{r} \cong (\mathbf{K}^{-1} + \omega^2 \mathbf{K}^{-1} \mathbf{M} \mathbf{K}^{-1}) \mathbf{B}^T \mathbf{p} \quad (20)$$

Substitution of the aforesaid relationship into the lower partition of Eq. (4) results in the subsequent equation

$$(\omega^4 \mathbf{S} \mathbf{M} \mathbf{S}^T + \omega^2 (\mathbf{G} + \mathbf{G}_a) - \mathbf{H}) \mathbf{p} = \mathbf{0} \quad (21)$$

in which

$$\mathbf{S} = \mathbf{B} \mathbf{K}^{-1} \quad (22)$$

Obviously, neglecting the first term of Eq. (21) results in Eq. (9) which is one of the eigen-problems in ideal-coupled approach. This fact demonstrates that the second form of the ideal-coupled approach is a special case of the second quadratic ideal-coupled technique. The size of this quadratic eigen-problem is equal to the number of the unknown nodal pressures.

It should be noted that a $n \times n$ quadratic eigen-problem has $2n$ eigen-values. Based on the characteristics of the coefficient matrices, the eigen-values may be infinite or finite (Tisseur and Meerbergen 2001). The finite values may be real or complex. It is worthwhile to mention that the real values are the approximate natural frequencies of the dam-reservoir system, and the other values are fictitious.

The aforesaid two quadratic ideal-coupled eigen-value problems, i.e., Eqs. (16) and (21), can be written totally as the following forms

$$\begin{bmatrix} \omega^4 \mathbf{Q} \mathbf{G} \mathbf{Q}^T + \omega^2 (\mathbf{M} + \mathbf{M}_a) - \mathbf{K} & & \\ & \mathbf{0} & \\ & & \omega^4 \mathbf{S} \mathbf{M} \mathbf{S}^T + \omega^2 (\mathbf{G} + \mathbf{G}_a) - \mathbf{H} \end{bmatrix} \begin{bmatrix} \mathbf{r} \\ \mathbf{p} \end{bmatrix} = \begin{bmatrix} \mathbf{0} \\ \mathbf{0} \end{bmatrix} \quad (23)$$

or

$$\left(\omega^4 \begin{bmatrix} \mathbf{Q} \mathbf{G} \mathbf{Q}^T & \mathbf{0} \\ \mathbf{0} & \mathbf{S} \mathbf{M} \mathbf{S}^T \end{bmatrix} + \omega^2 \begin{bmatrix} \mathbf{M} + \mathbf{M}_a & \mathbf{0} \\ \mathbf{0} & \mathbf{G} + \mathbf{G}_a \end{bmatrix} - \begin{bmatrix} \mathbf{K} & \mathbf{0} \\ \mathbf{0} & \mathbf{H} \end{bmatrix} \right) \begin{bmatrix} \mathbf{r} \\ \mathbf{p} \end{bmatrix} = \begin{bmatrix} \mathbf{0} \\ \mathbf{0} \end{bmatrix} \quad (24)$$

The solution of this combined symmetric eigen-problem can be obtained by solving two separate quadratic eigen-value problems. By neglecting $\omega^4 \mathbf{Q} \mathbf{G} \mathbf{Q}^T$ and $\omega^4 \mathbf{S} \mathbf{M} \mathbf{S}^T$ terms, this relationship converted into Eq. (12). Additionally, the original eigen-problem (Eq. (4)) can be transformed into a definite quadratic eigen-problem by multiplying the first its line by ω^2 (Kostic and Sikalo 2015). This nonlinear problem has the subsequent appearance

$$\left(\omega^4 \begin{bmatrix} \mathbf{M} & \mathbf{0} \\ \mathbf{0} & \mathbf{0} \end{bmatrix} + \omega^2 \begin{bmatrix} -\mathbf{K} & \mathbf{B}^T \\ \mathbf{B} & \mathbf{G} \end{bmatrix} - \begin{bmatrix} \mathbf{0} & \mathbf{0} \\ \mathbf{0} & \mathbf{H} \end{bmatrix} \right) \begin{bmatrix} \mathbf{r} \\ \mathbf{p} \end{bmatrix} = \begin{bmatrix} \mathbf{0} \\ \mathbf{0} \end{bmatrix} \quad (25)$$

This equation is an exact quadratic form of the eigen-value problem governing the free vibration of the dam-reservoir system.

4. Solving the quadratic eigen-problem

It should be reminded that the common scheme for the numerical solution of the standard eigen-problem (SEP), and the generalized one (GEP) is to reduce the matrices

involved to some simpler forms, which reveal the eigen-values. Unfortunately, these forms cannot be developed for nonlinear eigen-problems. Numerical strategies utilized for solving the quadratic eigen-problem (QEP) break into two categories: those that solve the quadratic eigen-problem directly, and those that work with the linearized forms (Afolabi 1987, Tisseur and Meerbergen 2001, Mackey *et al.* 2006). The latter technique, computes the simple forms to reveal the eigen-values and eigen-vectors directly. In what follows, these two types of approaches are briefly introduced. Moreover, a novel special-purpose eigen-value solution routine is developed for the proposed quadratic ideal-coupled formulations, which is presented in section 5.

4.1 Direct methods

It is worthwhile to highlight that most of the numerical procedures which deal directly with the quadratic eigen-problems are the variants of Newton's methods. These strategies calculate one eigen-pair at a time. Their rate of convergence is extensively dependent on the closeness of the starting guess to the actual solution. In practice, there is no guarantee that the technique will converge to the desired eigen-value even for a suitable initial guess. Newton's approaches are thoroughly investigated in Refs. (Higham and Kim 2001, Tisseur and Meerbergen 2001, Long *et al.* 2008).

4.2 Linearization method

The classical and most extensively utilized method to solve quadratic eigen-problems is linearization. In this process, a $n \times n$ quadratic eigen-problem can be transformed into a $2n \times 2n$ linear eigen-value problem. Consequently, it is possible to employ common linear eigen-solvers incorporated in commercial and noncommercial software packages. The eigen-values of the quadratic eigen-problem are similar to its linear form. Furthermore, its eigen-vectors can be achieved from the corresponding linear problem. It should be mentioned that various linear forms are available for a given QEP, based on the characteristics of the coefficient matrices. A drawback of this technique is that its dimension is twice of the original quadratic eigen-problem.

Herein, suitable symmetric linear forms of the quadratic ideal-coupled eigen-value problems are introduced, based on the linear forms presented in Ref. (Mackey *et al.* 2006). Recall that; other linearizations can be employed. The suggested linearization of the first quadratic ideal-coupled problem has the subsequent shape

$$\left(\omega^2 \begin{bmatrix} \mathbf{Q}\mathbf{G}\mathbf{Q}^T & \mathbf{Q}\mathbf{G}\mathbf{Q}^T \\ \mathbf{Q}\mathbf{G}\mathbf{Q}^T & \mathbf{M} + \mathbf{M}_a + \mathbf{K} \end{bmatrix} + \begin{bmatrix} \mathbf{M} + \mathbf{M}_a - \mathbf{Q}\mathbf{G}\mathbf{Q}^T & -\mathbf{K} \\ -\mathbf{K} & -\mathbf{K} \end{bmatrix} \right) \begin{bmatrix} \mathbf{r} \\ \bar{\mathbf{r}} \end{bmatrix} = \begin{bmatrix} \mathbf{0} \\ \mathbf{0} \end{bmatrix} \quad (26)$$

In this relation, $\bar{\mathbf{r}}$ includes fictitious entries. The dimension of this linear eigen-problem is twice of the unknown nodal displacements. Moreover, it is clear that the coefficient matrices are symmetric. Furthermore, it is

recommended that the next linearization should be used for the second quadratic ideal-coupled problem

$$\left(\omega^2 \begin{bmatrix} \mathbf{S}\mathbf{M}\mathbf{S}^T & \mathbf{S}\mathbf{M}\mathbf{S}^T \\ \mathbf{S}\mathbf{M}\mathbf{S}^T & \mathbf{G} + \mathbf{G}_a + \mathbf{H} \end{bmatrix} + \begin{bmatrix} \mathbf{G} + \mathbf{G}_a - \mathbf{S}\mathbf{M}\mathbf{S}^T & -\mathbf{H} \\ -\mathbf{H} & -\mathbf{H} \end{bmatrix} \right) \begin{bmatrix} \mathbf{p} \\ \bar{\mathbf{p}} \end{bmatrix} = \begin{bmatrix} \mathbf{0} \\ \mathbf{0} \end{bmatrix} \quad (27)$$

where $\bar{\mathbf{p}}$ contains fictitious entries. It is worthwhile to remark that the dimension of this problem is equal to the twice of the unknown nodal pressures. Similarly, the coefficient matrices are symmetric. Note that; these linear eigen-problems can be easily solved with the help of common linear symmetric eigen-value solution routines.

It is worth emphasizing that the exact quadratic form of the original eigen-problem (Eq. (24)) can be linearized in similar fashion. The dimension of the achieved eigen-value problem equals to the twice of the number of dam-reservoir system's degrees of freedom. As a result, the actual quadratic form requires more computational effort in comparison to the quadratic ideal-coupled eigen-value problems.

5. Generalized subspace method

Up to now, various algorithms have been presented for estimation of the natural frequencies and mode shapes of the linear symmetric eigen-problems. One of the well-known schemes widely used is named subspace iteration technique developed by Bathe (1996). This strategy is suitable for the finite element model of the huge structures (ADINA 2011). By this way, any arbitrary number of structural eigenvalues and eigenvectors can be obtained. Herein, this famous tactic is generalized for solving the quadratic ideal-coupled problems.

In each iteration of the suggested approach, a set of vectors are obtained. Number of these vectors are less than the size of the initial quadratic problem. The main problem is projected into the corresponding vector space. In this way, a smaller quadratic eigen-value problem is achieved. Then, it is linearized in a similar fashion to the previous sub-section. Afterwards, the common linear symmetric eigen-value solution routines are employed for solving this smaller problem. Its eigen-pairs are the approximations of the eigen-values and eigen-vectors of the initial quadratic eigen-problem. Finally, the eigen-pairs of the projected eigen-problem converges to the eigen-values and eigen-vectors of the initial quadratic one. It is worthwhile to mention that the decoupled mode shapes are utilized for forming the starting set of vectors, which establish the basis of the vector space in the first iteration. In Tables 1 and 2, the steps of this algorithm are presented for eigen-problems introduced in Eqs. (16) and (21), respectively.

It should be mentioned that $MaxIter$ and ε denotes the maximum allowable iteration and error. Moreover, vectors \mathbf{X}_F and \mathbf{X}_S finally converge to the pressure and displacement mode shapes, respectively.

Table 1 The algorithm of the generalized subspace method for eigen-problem presented in Eq. (16)

<p>Initialization</p> <p>ndm = Number of desired mode shapes</p> <p>Establish ndm starting vectors and save in \mathbf{X}_s^0</p> <p>Set ε and $MaxIter$</p> <p>Calculate the inverse of the stiffness matrix</p> <p>Iterations</p> <p>Do $k = 1, MaxIter$</p> $\bar{\mathbf{X}}_s = \mathbf{K}^{-1}(\mathbf{M} + \mathbf{M}_a)\mathbf{X}_s^{k-1}$ $\mathbf{K}^* = \bar{\mathbf{X}}_s^T \mathbf{K} \bar{\mathbf{X}}_s$ $\mathbf{M}^* = \bar{\mathbf{X}}_s^T \mathbf{M} \bar{\mathbf{X}}_s$ $\mathbf{M}_a^* = \bar{\mathbf{X}}_s^T \mathbf{M}_a \bar{\mathbf{X}}_s$ $(\mathbf{Q}\mathbf{G}\mathbf{Q}^T)^* = \bar{\mathbf{X}}_s^T (\mathbf{Q}\mathbf{G}\mathbf{Q}^T) \bar{\mathbf{X}}_s$ <p>Linearize and solve the projected quadratic eigen-problem</p> $\left[\omega^4 (\mathbf{Q}\mathbf{G}\mathbf{Q}^T)^* + \omega^2 (\mathbf{M}^* + \mathbf{M}_a^*) - \mathbf{K}^* \right] \mathbf{E}_s = \mathbf{0}$ $\mathbf{X}_s^k = \bar{\mathbf{X}}_s \mathbf{E}_s$ <p>Check for convergence</p> $\left \frac{\omega_i^k - \omega_i^{k-1}}{\omega_i^k} \right \leq \varepsilon, \text{ for } i=1,2,\dots,ndm$ <p>If all required eigen-values are converged, the iterations are stopped.</p> <p>End</p>

Table 2 The algorithm of the generalized subspace method for eigen-problem presented in Eq. (21)

<p>Initialization</p> <p>ndm = Number of desired mode shapes</p> <p>Establish ndm starting vectors and save in \mathbf{X}_F^0</p> <p>Set ε and $MaxIter$</p> <p>Calculate the inverse of the generalized stiffness matrix of the fluid domain</p> <p>Iterations</p> <p>Do $k = 1, MaxIter$</p> $\bar{\mathbf{X}}_F = \mathbf{H}^{-1}(\mathbf{G} + \mathbf{G}_a)\mathbf{X}_F^{k-1}$ $\mathbf{H}^* = \bar{\mathbf{X}}_F^T \mathbf{H} \bar{\mathbf{X}}_F$ $\mathbf{G}^* = \bar{\mathbf{X}}_F^T \mathbf{G} \bar{\mathbf{X}}_F$ $\mathbf{G}_a^* = \bar{\mathbf{X}}_F^T \mathbf{G}_a \bar{\mathbf{X}}_F$ $(\mathbf{S}\mathbf{M}\mathbf{S}^T)^* = \bar{\mathbf{X}}_F^T (\mathbf{S}\mathbf{M}\mathbf{S}^T) \bar{\mathbf{X}}_F$ <p>Linearize and solve the projected quadratic eigen-problem</p> $\left[\omega^4 (\mathbf{S}\mathbf{M}\mathbf{S}^T)^* + \omega^2 (\mathbf{G}^* + \mathbf{G}_a^*) - \mathbf{H}^* \right] \mathbf{E}_F = \mathbf{0}$ $\mathbf{X}_F^k = \bar{\mathbf{X}}_F \mathbf{E}_F$ <p>Check for convergence</p> $\left \frac{\omega_i^k - \omega_i^{k-1}}{\omega_i^k} \right \leq \varepsilon, \text{ for } i=1,2,\dots,ndm$ <p>If all required eigen-values are converged, the iterations are stopped.</p> <p>End</p>

6. Modeling and the basic parameters

As previously mentioned, finite element method was employed for the main part of the analysis technique in the present study. Many other works conducted recently in this field (Ghaemian and Ghobarah 1998, Sheibany and Ghaemian 2006, Mirzabozorg *et al.* 2010, Aftabi and Lotfi 2011). To reach this goal, a computer program was developed according to the theories explained in this article. The solid finite elements are applied for modeling the dam, and the reservoir is discretized by the fluid finite elements. The coupled method, decoupled approach, ideal-coupled technique and new quadratic ideal-coupled strategy are the available options for the analysis tool. These schemes were explained in the previous sections in detail. The eigen-solver used for the decoupled and ideal-coupled approaches is the linear symmetric subspace iteration tactic (Bathe 1996) which is denoted by SS in the following sections. It should be reminded that the true coupled problem is non-symmetric. As a result, the pseudo symmetric subspace iteration scheme (Arjmandi and Lotfi 2011) is applied for solving this problem. For brevity, this eigen-solver is abbreviated by PS. Moreover, two methods are employed for the quadratic eigen-value problems. The first one takes advantage of linearization and symmetric subspace iteration strategy (Bathe 1996), while the second one applies the suggested generalized subspace iteration algorithm. In this work, these two eigen-value solution routines are shown by

LS and GS, respectively.

In what follows, the free vibration analysis of Morrow Point arch dam is conducted with the help of the aforesaid methods. Based on the outcomes, the accuracy and consumed time of these schemes are compared. For this purpose, error and time indices are defined (Rezaiee-Pajand and Kazemiyani 2014, Rezaiee-Pajand *et al.* 2014). The following expressions mathematically demonstrate these indices, respectively

$$EI_i = 100 \times \left(\frac{1}{ndm} \sum_{j=1}^{ndm} \left| \frac{f_{exact}^j - f_i^j}{f_{exact}^j} \right| \right) \quad (28)$$

$$TI_i = 100 \times \frac{T_{\min}}{T_i} \quad (29)$$

where f_i^j and f_{exact}^j denote the j -th natural frequency of the i -th method and the true coupled one, correspondingly. Moreover, ndm is the number of computed natural frequencies. In addition, the consumed time of the fastest technique and the i -th scheme are shown by T_{\min} and T_i , respectively.

6.1 Model

In this study, a symmetric model of Morrow Point arch

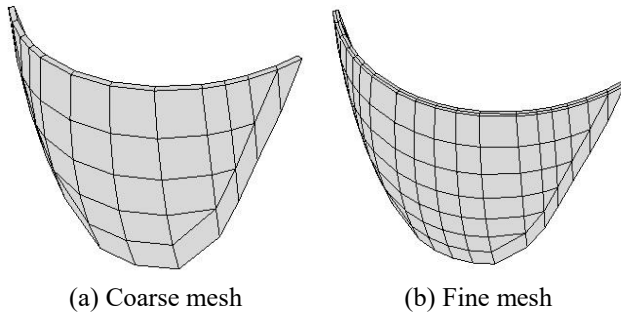


Fig. 1 Finite element meshes of the dam body

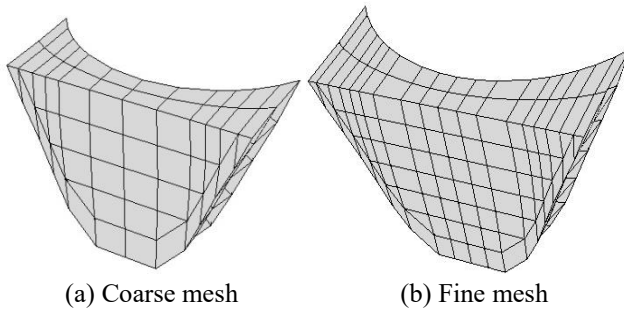


Fig. 2 Discretization of the water domain

dam on the rigid foundation is studied. The geometry of this dam is clearly available. To analyze this structure, two meshes are employed. In the first one, 40 isoparametric 20-node solid finite elements are used. This mesh has been widely employed by other researchers, and its high accuracy has been proved previously (Hall and Chopra 1983, Duron and Hall 1988, Noble 2002, Lotfi 2006, Lotfi 2007). Additionally, a fine mesh is also utilized (Arjmandi and Lotfi 2011). In this mesh, 168 isoparametric 20-node solid finite elements are applied. Fig. 1 demonstrates these meshes of the dam body.

According to different L/H parameters, various cases can be considered for the reservoirs. Herein, three cases are assessed. The water domain is considered as a region which extends to a specific length. It should be added that H is the dam height or the maximum water depth in the reservoir which is measured in upstream direction at the dam mid-crest point, and L denotes the water region length. In the first case, it is assumed that $L=0.2 H$, while $L=0.6 H$ in the second case. The third one deals with $L-H$. For both meshes, the water domain with $L=0.2 H$ is shown in Fig. 2.

6.2 Basic parameters

The concrete dam is presumed to be homogeneous with isotropic linear behavior, and it has the following main properties:

Elastic modulus (E_d)=27.5 GPa; Poisson's ratio = 0.2

Unit weight=24.8 kN/m³.

It should be mentioned that the impounded water is considered as inviscid and compressible fluid with a unit weight equal to 9.8 kN/m³, and pressure wave velocity $C=1440$ m/s.

6.3 Results

Table 3 The first five natural frequencies of the dam-reservoir system with the coarse mesh and $L=0.2 H$ according to the true coupled, the first case of the decoupled, ideal-coupled and quadratic ideal-coupled

Mode Number	Natural frequencies f_i (Hz) (Coarse mesh)			
	Decoupled (SS) (Lotfi 2005)	Ideal-coupled (SS) (Aftabi and Lotfi 2010)	Quadratic ideal-coupled (LS-GS) (Presented method)	True coupled system (PS) (Aftabi and Lotfi 2010)
	Dam	First ideal case (incompressible fluid assumption)	First quadratic ideal case	
1	3.75	2.57	2.29	2.19
2	4.20	2.82	2.76	2.76
3	6.05	4.15	3.85	3.63
4	6.71	4.80	4.68	4.65
5	7.69	5.95	5.54	5.23

Table 4 The first five natural frequencies of the dam-reservoir system with the fine mesh and $L=0.2 H$ according to the true coupled, the first case of the decoupled, ideal-coupled and quadratic ideal-coupled

Mode Number	Natural frequencies f_i (Hz) (Fine mesh)			
	Decoupled (SS) (Lotfi 2005)	Ideal-coupled (SS)	Quadratic ideal-coupled (LS-GS) (Presented method)	True coupled system (PS)
	Dam	First ideal case (incompressible fluid assumption)	First quadratic ideal case	
1	3.68	2.54	2.28	2.16
2	4.19	2.75	2.70	2.69
3	5.93	4.07	3.84	3.60
4	6.69	4.68	4.59	4.54
5	7.43	5.70	5.58	5.05

In this section, the natural frequencies and mode shapes of the dam-reservoir system are computed by employing the aforesaid four approaches. The obtained results are compared to highlight the robustness and efficiency of authors' schemes. Now, for the coarse and fine meshes with $L=0.2 H$, the first five natural frequencies of the following four methods: (1) decoupled, (2) ideal-coupled, (3) quadratic ideal-coupled and (4) true coupled are computed. Recall that each formulation consists of two eigen-problems, and consequently, includes two sets of the modes, except for the true coupled method. It is worthwhile to mention that the set of mode shapes related to the nodal displacements can be achieved by solving the first eigen-value problems, while the corresponding set of mode shapes associated with the nodal pressures can be obtained by solving the second eigen-value problems. Note that; the nodal pressures are the unknowns of fluid elements' nodes, and the nodal displacements are the unknowns of the dam. Accordingly, the frequencies of the first eigen-problem are presented in Tables 3 and 4, respectively.

Herein, the frequencies of the second eigen-problems are presented in Table 5 and 6, respectively.

Table 5 The first five natural frequencies of the dam-reservoir system with the coarse mesh and $L=0.2 H$ according to the true coupled, the second case of the decoupled, ideal-coupled and quadratic ideal-coupled

Mode Number	Natural frequencies f_i (Hz) (Coarse mesh)			
	Decoupled (SS) (Lotfi 2005)	Ideal-coupled (SS) (Aftabi and Lotfi 2010)	Quadratic ideal-coupled (LS-GS) (Presented method)	True coupled system (PS) (Aftabi and Lotfi 2010)
	Reservoir	Second ideal case (massless solid assumption)	First quadratic ideal case	
1	3.42	2.32	2.21	2.19
2	6.59	3.75	3.07	2.76
3	7.87	4.93	4.11	3.63
4	10.21	6.53	5.30	4.65
5	11.73	6.75	5.83	5.23

Table 6 The first five natural frequencies of the dam-reservoir system with the fine mesh and $L=0.2 H$ according to the true coupled, the second case of the decoupled, ideal-coupled and quadratic ideal-coupled

Mode Number	Natural frequencies f_i (Hz) (Fine mesh)			
	Decoupled (SS)	Ideal-coupled (SS)	Quadratic ideal-coupled (LS-GS) (Presented method)	True coupled system (PS)
	Reservoir	Second ideal case (massless solid assumption)	First quadratic ideal case	
1	3.42	2.29	2.19	2.16
2	6.53	3.63	2.99	2.69
3	7.85	4.87	4.08	3.60
4	10.05	6.36	5.17	4.54
5	11.73	6.52	5.64	5.05

Based on these outcomes, it is clear that the true coupled natural frequencies are smaller than two sets of natural frequencies obtained from the decoupled, ideal-coupled or quadratic ideal-coupled technique. However, it is obvious that the natural frequencies related to the ideal-coupled and quadratic ideal-coupled schemes are getting closer to the true coupled ones, in comparison to the decoupled method. It should be mentioned that the first ideal-coupled strategy is a special case of the first quadratic ideal-coupled technique.

The first quadratic form is more accurate than the first ideal-coupled approach. Furthermore, the second ideal-coupled method is a special case of the second quadratic ideal-coupled technique. In comparison to the second ideal-coupled formulation, the second quadratic form leads to the natural frequencies closer to the true coupled approach. According to the results, it can be concluded that each quadratic ideal-coupled strategy has better accuracy than its corresponding ideal-coupled scheme. At this stage, the aforesaid four algorithms are employed for calculating the natural frequencies of the case in which $L=0.6 H$. For brevity, the results of the fine mesh are neglected. The obtained results are available in Tables 7 and 8.

According to the results of Tables 7 and 8, it is observed that the true coupled natural frequencies are smaller than

Table 7 The first five natural frequencies of the dam-reservoir system with the coarse mesh and $L=0.6 H$ according to the true coupled, the first case of the decoupled, ideal-coupled and quadratic ideal-coupled

Mode Number	Natural frequencies f_i (Hz) (Fine mesh)			
	Decoupled (SS)	Ideal-coupled (SS)	Quadratic ideal-coupled (LS-GS) (Presented method)	True coupled system (PS)
	Dam	First ideal case (incompressible fluid assumption)	First quadratic ideal case	
1	3.75	2.94	2.85	2.56
2	4.20	3.09	2.91	2.91
3	6.05	4.68	4.22	3.62
4	6.71	4.93	4.79	4.74
5	7.69	6.31	6.06	5.77

Table 8 The first five natural frequencies of the dam-reservoir system with the coarse mesh and $L=0.6 H$ according to the true coupled, the second case of the decoupled, ideal-coupled and quadratic ideal-coupled

Mode Number	Natural frequencies f_i (Hz) (Fine mesh)			
	Decoupled (SS)	Ideal-coupled (SS)	Quadratic ideal-coupled (LS-GS) (Presented method)	True coupled system (PS)
	Reservoir	Second ideal case (massless solid assumption)	First quadratic ideal case	
1	3.13	2.71	2.61	2.56
2	7.00	4.30	3.36	2.91
3	7.83	5.28	4.21	3.62
4	9.63	6.86	5.48	4.74
5	10.53	7.15	6.42	5.77

Table 9 The first five natural frequencies of the dam-reservoir system with the coarse mesh and $L=H$ according to the true coupled, the first case of the decoupled, ideal-coupled and quadratic ideal-coupled

Mode Number	Natural frequencies f_i (Hz) (Fine mesh)			
	Decoupled (SS)	Ideal-coupled (SS)	Quadratic ideal-coupled (LS-GS) (Presented method)	True coupled system (PS)
	Dam	First ideal case (incompressible fluid assumption)	First quadratic ideal case	(Arjmandi and Lotfi 2011)
1	3.75	2.94	2.91	2.68
2	4.20	3.15	2.98	2.92
3	6.05	4.75	4.34	3.53
4	6.71	5.00	4.80	4.75
5	7.69	6.32	6.08	5.14

decoupled, ideal-coupled and quadratic ideal-coupled ones. Additionally, the decoupled approach is the least accurate method. Moreover, each quadratic ideal-coupled strategy is more accurate than its corresponding ideal-coupled scheme.

Now, the aforesaid four tactics are similarly utilized for calculating the natural frequencies of the case in which the coarse mesh with $L=H$ is employed. The achieved results

Table 10 The first five natural frequencies of the dam-reservoir system with the coarse mesh and $L=H$ according to the true coupled, the second case of the decoupled, ideal-coupled and quadratic ideal-coupled

Mode Number	Natural frequencies f_i (Hz) (Fine mesh)			
	Decoupled (SS)	Ideal-coupled (SS)	Quadratic ideal-coupled (LS-GS) (Presented method)	True coupled system (PS)
	Reservoir	Second ideal case (massless solid assumption)	First quadratic ideal case	(Arjmandi and Lotfi 2011)
1	3.09	2.81	2.72	2.68
2	6.21	4.33	3.38	2.92
3	7.08	4.84	4.03	3.53
4	7.83	6.09	5.37	4.75
5	8.66	6.89	5.62	5.14

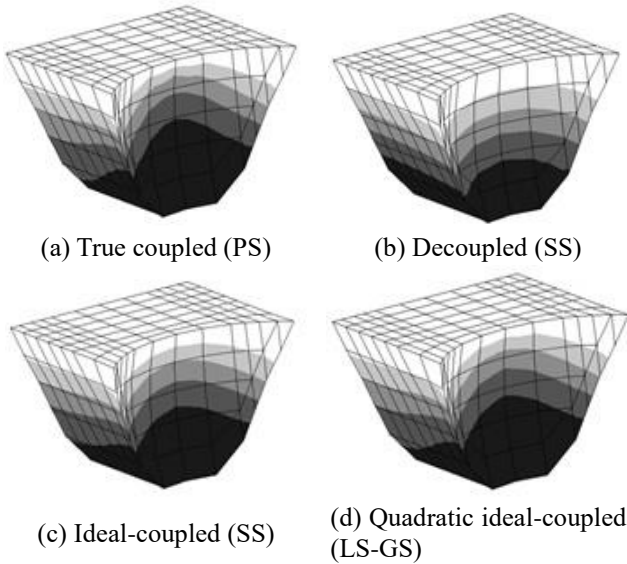


Fig. 3 First pressure mode shape of the coarse model of the dam-reservoir system with $L=H$

are listed in Tables 9 and 10.

Based on the results demonstrated in Tables 9 and 10, it is observed that the true coupled natural frequencies are smaller than decoupled, ideal-coupled and quadratic ideal-coupled ones. Additionally, the decoupled algorithm leads to the least accurate natural frequencies. Besides, each quadratic ideal-coupled strategy is more accurate than its corresponding ideal-coupled technique. It is clear that, the quadratic ideal-coupled formulation performs more accurately than other methods.

Herein, the first mode shape of the dam-reservoir system with $L=H$ is obtained by using the four aforementioned approaches. For brevity, the mode shapes of the fine model are not presented. It should be added that the mode shapes of the fine and coarse model are the same. The achieved mode shapes corresponding to the fluid domain are demonstrated in Fig. 3.

It can be observed that the quadratic ideal-coupled mode shape is more similar to the true coupled one, although the four pressure distributions are analogous. At the next stage,

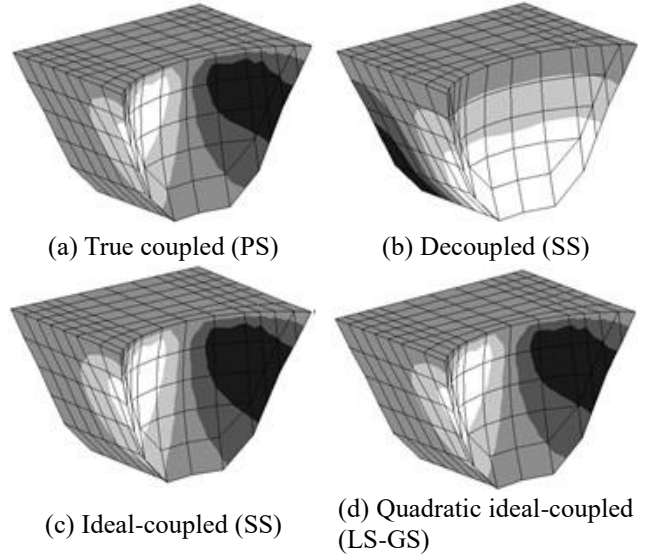


Fig. 4 Second pressure mode shape of the coarse model of the dam-reservoir system with $L=H$

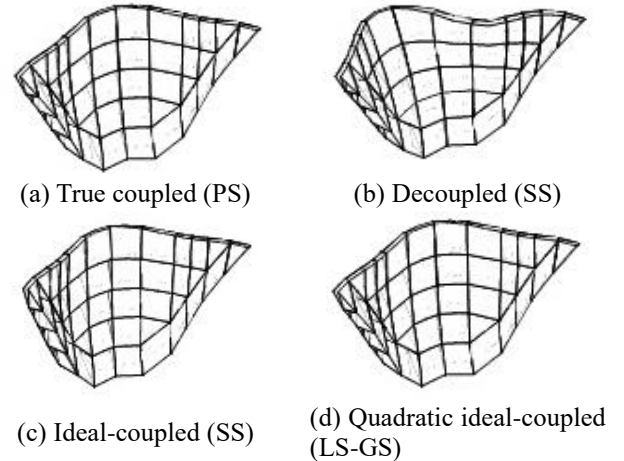


Fig.5 First mode shape of the dam

the second mode shape of the aforementioned system is presented in Fig. 4. It should be reminded that only the fluid domain is shown.

Obviously, the decoupled mode shape is totally different from the true coupled mode shape. Additionally, the ideal-coupled mode shape is not completely the same as the true one. It is clear that the quadratic ideal-coupled pressure mode shape is the closest mode shape to the actual one, in comparison to decoupled and ideal-coupled mode shapes.

Now, the first mode shape of the dam is presented in Fig. 5.

Clearly, the decoupled mode shape is totally different from the true coupled mode shape. Additionally, the ideal-coupled and quadratic ideal-coupled mode shapes are similar to the actual one. In Fig. 6, the second mode shape of the dam is shown.

Based on these figures, the suggested tactic is successful in obtaining the second mode shape of the dam.

For the above-cited dam-reservoir systems, Tables 11 and 12 illustrate the error and time indices of the decoupled, ideal-coupled, quadratic ideal-coupled and true coupled

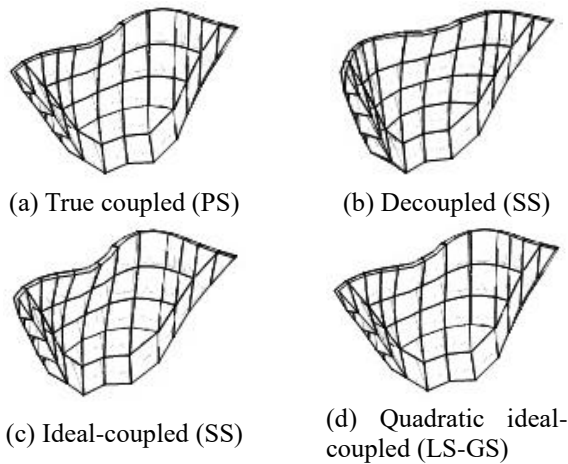


Fig.6 Second mode shape of the dam

Table 11 The error indices of the decoupled, ideal coupled and quadratic ideal-coupled methods

Case	Decoupled (SS)	Ideal-coupled (SS)	Quadratic Ideal-coupled (LS-GS)
Coarse mesh with $L/H=0.2$	83.70	19.80	6.80
Fine mesh with $L/H=0.2$	85.81	19.43	7.56
Coarse mesh with $L/H=0.6$	69.76	23.18	9.46
Coarse mesh with $L/H=1$	60.79	23.29	10.67

approaches, correspondingly.

Accordingly, it is obvious that the most accurate tactic is authors' technique. Moreover, the error index of the decoupled method is higher than those of others in all numerical examples. As it was expected, the least accurate decoupled strategy is the fastest one. The ideal-coupled method is ranked second. The quadratic ideal-coupled with GS is much faster than the true coupled with PS. Besides, the quadratic ideal-coupled with LS is the slowest one.

It is worthwhile to remind that the efficiency of a numerical method depends on both its consumed time and accuracy. Accordingly, the ideal-coupled scheme and quadratic ideal-coupled technique with GS perform more efficiently in comparison to the others.

7. Conclusions

The eigen-problem of the dam-reservoir system is generally not symmetric, and it cannot be solved with the help of common linear symmetric eigen-value solution routines. To overcome this difficulty, quadratic ideal-coupled scheme is suggested in the present work which could be an extension of earlier ones (Lotfi 2005, Aftabi and Lotfi 2010). In this tactic, two quadratic eigen-problems are required to be solved. Their eigen-pairs can be computed with the help of common linear symmetric eigen-value solution routines if their linearized forms are applied. Additionally, a novel efficient algorithm is proposed for solving the corresponding quadratic eigen-problems. From

Table 12 The time indices of the decoupled, ideal coupled and quadratic ideal-coupled methods

Case	Decoupled	Ideal-coupled	Quadratic Ideal-coupled		True coupled
	SS	SS	LS	GS	PS
Coarse mesh with $L/H=0.2$	100	94.13	1.94	36.39	4.04
Fine mesh with $L/H=0.2$	100	84.60	2.94	37.10	6.27
Coarse mesh with $L/H=0.6$	100	89.43	2.09	33.10	4.52
Coarse mesh with $L/H=1$	100	90.67	2.27	33.77	4.36

accuracy point of view, this strategy is compared with the decoupled and ideal-coupled approaches proposed in the previous studies. To reach this goal, the Morrow point concrete arch dam with its reservoir is envisaged as an example. It should be reminded that two sets of the natural frequencies exist for the decoupled, ideal-coupled and quadratic ideal-coupled methods. The first set of the quadratic ideal-coupled technique is closer to the true coupled natural frequencies, in comparison to the first set of the decoupled and ideal-coupled tactics. Furthermore, the second set of the quadratic ideal-coupled strategy is more accurate than the corresponding set of other two schemes. In addition, the first two mode shapes achieved from the aforesaid three methods are compared. It is observed that the quadratic ideal-coupled mode shapes are more analogous to the true ones than those of other algorithms. Moreover, the quadratic ideal-coupled scheme with the suggested eigen-solver algorithm is faster than the true coupled one with the pseudo symmetric method. However, it requires more time in comparison to the decoupled and ideal-coupled techniques.

References

- ADINA (2011), On the use of the subspace iteration method, www.adina.com
- Afolabi, D. (1987), "Linearization of the quadratic eigenvalue problem", *Comput. Struct.*, **26**(6), 1039-1040.
- Aftabi, S.A. and Lotfi, V. (2010), "Dynamic analysis of concrete arch dams by ideal-coupled modal approach", *Eng. Struct.*, **32**(5), 1377-1383.
- Aftabi, S.A. and Lotfi, V. (2011), "An effective procedure for seismic analysis of arch dams including dam-reservoir-foundation interaction effects", *J. Earthq. Eng.*, **15**(7), 971-988.
- Arjmandi, S.A. and Lotfi, V. (2011), "Computing mode shapes of fluid-structure systems using subspace iteration methods", *Sci. Iran*, **18**(6), 1159-1169.
- Bathe, K.J. (1996), *Finite Element Procedure*, Prentice-Hall, INC., Upper Saddle River, New Jersey, USA.
- Bathe, K.J. and Hahn, W.F. (1979), "On transient analysis of fluid-structure systems", *Comput. Struct.*, **10**, 383-391.
- Bouaanani, N. and Lu, F.Y. (2009), "Assessment of potential-based fluid finite elements for seismic analysis of dam-reservoir systems", *Comput. Struct.*, **87**, 206-224.
- Chopra, A.K. (2012), "Earthquake analysis of arch dams: factors to be considered", *J. Struct. Eng.*, ASCE, **138**, 205-214.
- Duron, Z.H. and Hall, J.F. (1988), "Experimental and finite

- element studies of the forced vibration response of Morrow Point dam”, *Earthq. Eng. Struct. D.*, **16**, 1021-1039.
- Everstine, G.C. (1981), “A symmetric potential formulation for fluid structure interaction”, *J. Sound Vib.*, **79**(1), 157-160.
- Felippa, C.A. (1985), “Symmetrization of the contained compressible-fluid vibration eigenproblem”, *Commun. Appl. Numer. M.*, **1**, 241-247.
- Felippa, C.A. (1988), “Symmetrization of coupled eigenproblems by eigenvector augmentation”, *Commun. Appl. Numer. M.*, **4**, 561-563.
- Geradin, M., Robert, G. and Huck, A. (1984), “Eigenvalue analysis and transient response of fluid-structure interaction problems”, *Eng. Comput.*, **1**, 151-160.
- Ghaemian, M. and Ghobarah, A. (1998), “Staggered solution schemes for dam reservoir interaction”, *J. Fluid Struct.*, **12**, 933-948.
- Hall, J.F. and Chopra, A.K. (1983), “Dynamic analysis of arch dams including hydrodynamic effects”, *J. Eng. Mech. Div.*, ASCE, **109**(1), 149-163.
- Higham, N.J. and Kim, H.M. (2001), “Solving a quadratic matrix equation by Newton’s method with exact line searches”, *SIAM J. Matrix Anal. A.*, **23**(2), 303-316.
- Hojati, M. and Lotfi, V. (2011), “Dynamic analysis of concrete gravity dams utilizing two-dimensional modified efficient fluid hyper-element”, *Adv. Struct. Eng.*, **14**(6), 1093-1106.
- Kayser-Herold, O. and Matthies, H.G. (2005), “Least squares finite element methods for fluid-structure interaction problems”, *Comput. Struct.*, **83**, 191-207.
- Kostic, A. and Sikalo, S. (2015), “Definite quadratic eigenvalue problems”, *Procedia Eng.*, **100**, 56-63.
- Long, J.H., Hu, X.Y. and Zhang, L. (2008), “Improved Newton’s method with exact line searches to solve quadratic matrix equation”, *J. Comput. Appl. Math.*, **222**, 645-654.
- Lotfi, V. (2005), “Frequency domain analysis of concrete arch dams by decoupled modal approach”, *Struct. Eng. Mech.*, **21**(4), 423-435.
- Lotfi, V. (2006), “An efficient three-dimensional fluid hyper-element for dynamic analysis of concrete arch dams”, *Struct. Eng. Mech.*, **24**(6), 683-698.
- Lotfi, V. (2007), “Direct frequency domain analysis of concrete arch dams based on FE-BE procedure”, *Struct. Eng. Mech.*, **26**(4), 363-376.
- Mackey, D.S., Mackey, N., Mehl, C. and Mehrmann, V. (2006), “Vector space of linearizations for matrix polynomials”, *SIAM J. Matrix Anal. A.*, **28**(4), 971-1004.
- Mirzabozorg, H., Varmazyari, M. and Ghaemian, M. (2010), “Dam-reservoir-massed foundation system and travelling wave along reservoir bottom”, *Soil Dyn. Earthq. Eng.*, **30**, 746-756.
- Morand, H. and Ohayon, R. (1979), “Substructure variational analysis of the vibrations of coupled fluid-structure systems. Finite element results”, *Int. J. Numer. Meth. Eng.*, **14**, 741-755.
- Noble, C.R. (2002), “Seismic analysis of Morrow point dam”, *Workshop on Non-Linear Structural Analysis of Concrete Dams and Concrete Appurtenances to Dams*, Denver, Colorado, USA.
- Olson, L.G. and Bathe, K.J. (1985), “Analysis of fluid structure interactions. A direct symmetric coupled formulation based on the fluid velocity potential”, *Comput. Struct.*, **21**, 21-32.
- Olson, L.G. and Vandini, T. (1989), “Eigenproblems from finite element analysis of fluid-structure interactions”, *Comput. Struct.*, **33**(3), 679-687.
- Rezaiee-Pajand, M., Aftabi, S.A. and Kazemiyani, M.S. (2016), “Analytical solution for free vibration of flexible 2D rectangular tanks”, *Ocean Eng.*, **122**, 118-135.
- Rezaiee-Pajand, M. and Kazemiyani, M.S. (2014), “Damage identification of 2D and 3D trusses by using complete and incomplete noisy measurements”, *Struct. Eng. Mech.*, **52**(1), 149-172.
- Rezaiee-Pajand, M., Kazemiyani, M.S. and Aftabi, S.A. (2014), “Static damage identification of 3D and 2D frames”, *Mech. Bas. Des. Struct.*, **42**, 70-96.
- Samii, A. and Lotfi, V. (2007), “Comparison of coupled and decoupled modal approaches in seismic analysis of concrete gravity dams in time domain”, *Finite Elem. Anal. Des.*, **43**, 1003-1012.
- Sandberg, G. (1995), “A new strategy for solving fluid-structure problems”, *Int. J. Numer. Meth. Eng.*, **38**, 357-370.
- Sheibany, F. and Ghaemian, M. (2006), “Effects of environmental action on thermal stress analysis of karaj concrete arch dam”, *J. Eng. Mech.*, ASCE, **132**(5), 532-544.
- Tisseur, F. and Meerbergen, K. (2001), “The quadratic eigenvalue problem”, *SIAM Rev.*, **43**(2), 235-286.
- Zienkiewicz, O.C. and Bettess, P. (1978), “Fluid-structure dynamic interaction and wave forces. An introduction to numerical treatment”, *Int. J. Numer. Meth. Eng.*, **13**, 1-16.

CC